*Romanian Reports in Physics, Vol. 64, No. 1, P. 105–115, 2012*

**CONDENSED MATTER**

# FORMATION OF FARADAY AND RESONANT WAVES IN DRIVEN BOSE-EINSTEIN CONDENSATES

MIHAELA-CARINA RAPORTARU[1,2]

[1]"Horia Hulubei" National Institute for Physics and Nuclear Engineering,
30 Reactorului, Magurele, 077125, Romania
[2]University of Bucharest, Faculty of Physics, Atomistilor 405, Magurele, Romania
*E-mail*: mraportaru@nipne.ro

*Received October 10, 2011*

*Abstract.* We introduce a variational method to describe the dynamics of cigar-shaped Bose-Einstein condensates of high density subject to periodic modulations of the radial component of the confining potential. The key ingredient of the variational treatment is the $q$-Gaussian radial envelope which describes the Thomas-Fermi regime of the condensate. A longitudinal surface wave of the type $(1+(u(t)+iv(t))\cos kz)$ is grafted to the ansatz to account for Faraday and resonant waves. Using the variational equations, we investigate the dynamics of a realistic condensate for frequencies close to the radial frequency of the trap and show the emergence of the Faraday waves excited outside of resonance and that of the resonant wave that appears straight on resonance.

*Key words*: Faraday waves, resonant wave, $q$-Gaussian ansatz.

## 1. INTRODUCTION

A period of seven decades separates the theoretical prediction that a dilute atomic gas will Bose-condense at very low temperatures from the land-marking experimental achievement of Bose-Einstein condensates (BECs) with $^{87}$Rb and $^{23}$Na atoms in 1995 [1]. There were very few signs along the way to suggest the almost unprecedented scientific effervescence that gathered scientists from fields as diverse as atomic and solid state physics on one end, and nonlinear and quantum optics at the other. Nonlinear scientists, in particular, have found in BECs their ideal testbed for nonlinear phenomena at large and there is now a long list of experimental results reinforced theoretically by supporting analytical results and extensive numerical simulations [2–4].

Extended parametric resonances are one of the recurrent themes in the dynamics of quantum gases. Following the inceptive investigations in Ref. [5] and the subsequent theoretical prediction of Faraday waves in parametrically driven BECs [6] they have received constant attention [7]. The experimental observation of Fara-

day waves in cigar-shaped $^{87}$Rb BECs [8] and $^{4}$He cells subject to vertical vibrations [9], and the achievement of periodic modulations of the scattering length of a $^{7}$Li BEC [10] represented a supplementary stimulus that greatly catalyzed investigations on this subject. A close look at the recent literature for bosonic systems shows a large number of publications on subjects as diverse as the nonlinear correction to the frequencies of the collective modes of a BEC [11], the path-integral formalism for the dynamics of bosonic gases (see Ref. [12] for a detailed overview), the parametric excitation of "scars" in BECs [13], the complete removal of excitations in BECs subject to time-dependent periodic potentials [14] and the formation of Faraday patterns in low-density, high-density and dipolar BECs [15–17].

Investigations into the properties of BECs loaded into optical lattices [18] have uncovered a wide range of nonlinear phenomena that includes loops in the condensate band structure, trains of solitons and period doubled states [19, 20]. The suppression of Faraday waves in BECs loaded into strong optical lattices, in particular, was shown through numerical simulations in Ref. [21] using mainly a homogeneous setting. On the fermionic side, the properties of Faraday waves in superfluid fermionic gases have been discussed in Refs. [22, 23] and the amplification of the spin-charge separation in one-dimensional fermionic systems by means of parametric resonances has been shown in Ref. [24].

The large number of theoretical investigations into the nonlinear dynamics of BECs stems from the well-established accuracy of the Gross-Pitaevskii (GP) equation that governs the $T = 0$ K dynamics of the condensate. A mathematically identical equation has been used in nonlinear optics to describe quasi-monochromatic wave trains propagating in nonlinear optical media and it has been shown that it supports numerous stable nonlinear waveforms in one-, two- and three-dimensional conservative [25] and dissipative [26] physical settings; for a comprehensive review see Ref. [27].

There is now a large number of numerical recipes that can solve the GP equation in one-, two- and three-dimensional settings (see, for instance, Ref. [28]), while for analytic results one can choose between effectively one- and two-dimensional non-polynomial Schrödinger equations [29,30], discrete nonlinear Schrödinger equations [31] and numerous variational treatments [32]. As most experimental setups use high-density condensates, the most attractive variational methods are those tailored around $q$-Gaussian functions [33–35] which are known to give the correct hydrodynamic description of the condensate [36]. These $q$-Gaussian variational treatments have had notable successes in describing the ground state properties of the condensate [33–35] along with its resonant and non-resonant dynamics [36], and, what is even more interesting, can describe the condensate midway between the low- and the high-density regime where all other methods fail.

In this work we extend a previous treatment of surface waves [37] to describe

the emergence of Faraday and resonant waves in driven Bose-Einstein condensates that have longitudinal homogeneity [38]. The key ingredient of the current treatment is the $q$-Gaussian transverse envelope which accurately describes the dynamics of BECs with large numbers of atoms an aspect that has been neglected in concurrent works [39]. A related treatment has been used in the past to investigate the dynamics of loosely bound two-dimensional solitons in BECs loaded into optical lattices [40]. The rest of the paper is structured as follows: In Section II we introduce the variational recipe and derive the Euler-Lagrange equations, while in Section III we present the numerical results. Finally, in Section IV we gather the main conclusions and present suggestions for future experiment.

## 2. VARIATIONAL TREATMENT

Starting from the Lagrangian density of a trapped BEC (written herein with $\hbar = m = 1$)

$$\mathcal{L}(\mathbf{r},t) = \frac{i}{2}\left(\psi(\mathbf{r},t)\frac{\partial\psi^*(\mathbf{r},t)}{\partial t} - \psi^*(\mathbf{r},t)\frac{\partial\psi(\mathbf{r},t)}{\partial t}\right) + \frac{1}{2}\left|\nabla\psi(\mathbf{r},t)\right|^2 + V(\mathbf{r},t)\left|\psi(\mathbf{r},t)\right|^2 + \frac{g(t)N}{2}\left|\psi(\mathbf{r},t)\right|^4 \quad (1)$$

and using the trial wave function

$$\psi(r,z,t) = \left[\frac{k\,(3-q)}{2\pi^2\,(2+u(t)^2+v(t)^2)\,w(t)^2}\right]^{1/2}\left[1-\frac{r^2\,(1-q)}{2w^2(t)}\right]^{1/1-q} \times \exp\left[ir^2\alpha(t)\right]\left[1+(u(t)+iv(t))\cos(kz)\right] \quad (2)$$

one can integrate out the radial and the longitudinal components which leads to the following Lagrangian

$$\begin{aligned} L(t) = &-\frac{2g\pi\rho(q-3)^2\left[8-3u^4(t)-8v^2(t)+3v^4(t)+6u^2(t)\left(4+v^2(t)\right)\right]}{16\pi^2(q-5)\left[2+u^2(t)+v^2(t)\right]^2 w_r^2(t)} \\ &+\frac{\Omega^2(t)w^2(t)}{4-2q}+\Bigg\{(6+2q)(q-2)+(q-2)v^2(t)(3-q) \\ &+k^2(1+q)w^2(t)-(4+q)\Big[2+v^2(t)w^4(t)\alpha^2(t) \\ &+u^2(t)(3-q)(2+q)+(1-q)w^2(t)\left[k^2(q-2)-4w^2(t)\alpha^2(t)\right]\Big]\Bigg\} \\ &\times\Bigg\{2(q-2)(1+q)\left[2+u^2(t)+v^2(t)\right]w^2(t) \end{aligned} \quad (3)$$

$$+\frac{-v(t)\dot{u}(t)+u(t)\dot{v}(t)}{2+u^2(t)+v^2(t)}-\frac{w^2(t)\dot{\alpha}(t)}{q-2}\Bigg\}^{-1}.$$

Our ansatz (and the ensuing Lagrangian) covers longitudinally-homogeneous, cigar-shaped BECs subject to isotropic transverse confinement. More refined treatments include a longitudinal envelope to cover the weak longitudinal trapping that exists in most experimental setups. In this work we have chosen to omit longitudinal envelopes of finite spatial extent due to the spurious resonances that appear between the length of the condensate and the period of the surface wave. Applying the Euler-Lagrange equations

$$\frac{\mathrm{d}}{\mathrm{d}t}\left(\frac{\partial L}{\partial \dot{y}}\right)-\frac{\partial L}{\partial y}=0, \tag{4}$$

with $y\in\{q,w,\alpha,v,u\}$ one obtains the following variational equations, namely

$$-\frac{(7-q)(3-q)\rho g}{2\pi(q-5)^2}-\frac{4}{(1+q)^2}+\frac{\Omega^2(t)w^4(t)}{(q-2)^2}=0 \tag{5}$$

for $q$ and

$$\begin{aligned}\dot{\alpha}(t)=\frac{1}{w(t)}(q-2)\Bigg(&\frac{g\,(q-3)^2\,\rho}{2\pi(5-q)w^3(t)}-\frac{\Omega^2(t)w(t)}{2-q}\\&-\frac{8w(t)\alpha^2(t)}{(q-2)}+\frac{4w^4(t)\alpha^2(t)}{(q-2)w^3(t)}+\frac{6-5q+q^2}{(q-2)(1+q)w^3(t)}\Bigg)\end{aligned} \tag{6}$$

$$\dot{w}(t)=2w(t)\alpha(t) \tag{7}$$

$$\dot{v}(t)=\frac{g(q-3)^2\rho u(t)}{\pi(q-5)w^2(t)}-\frac{k^2}{2}u(t) \tag{8}$$

$$\dot{u}(t)=\frac{k^2}{2}v(t) \tag{9}$$

for $w$, $\alpha$, $u$ and $v$, respectively. Equations (6)–(9) describe the dynamics of the bulk and the formation of the surface wave for a generic condensate, the radial density distribution of the bulk being set by $q$ through the algebraic constraint in equation (5). The algebraic nature of the constraint that sets the radial density distribution is due to $q$ not having a canonically conjugate variable (for example, a phase), which we have intentionally omitted for reasons of analytical tractability. In fact, the slightest change of the ansatz turns the Lagrangian analytically intractable and one is left only with direct variational methods which have the same lack of transparency as the numerical solution of the original GP equation. A detailed discussion on the solutions of equation (5) is presented in Ref. [36]. Here let us mention that for $q=1$

equation (6) reduces to

$$\dot{\alpha}(t) = \frac{g\rho}{4\pi w^4(t)} - \frac{\Omega^2(t)}{2} - 2\alpha^2(t) + \frac{1}{2w^4(t)} \tag{10}$$

which has been used in Ref. [38] to describe the formation of resonant waves in low-density condensates, while for $q = -1$ the last term in equation (6) becomes singular. This singularity corresponds to the divergence of the kinetic energy close to the surface of the condensate that is typical for the Thomas-Fermi approximation. The radial density distribution of the bulk has little impact on the formation of the longitudinal surface wave as one can see from the dynamics of $v(t)$ for $q = 1$

$$\dot{v}(t) = -\frac{g\rho u(t)}{\pi w^2(t)} - \frac{k}{2}u(t) \tag{11}$$

and $q = -1$

$$\dot{v}(t) = -\frac{8g\rho u(t)}{3\pi w^2(t)} - \frac{k^2}{2}u(t). \tag{12}$$

Outside of the radial resonance, that is $\omega \neq \Omega$, we can approximate the solution of (6) and (7) as

$$w(t) \approx \left[\frac{\left(6-5q+q^2\right)\left(g\rho(3+2q-q^2)+2\pi\left(5-q\right)\right)}{2\pi\Omega^2\left(5+4q-q^2\right)\left(1+\epsilon\sin t\omega\right)^2}\right]^{1/4}. \tag{13}$$

Using (13) in (8) we then recast equations (8) and (9) in the form of a generic Mathieu equation

$$\ddot{u}(t) + u(t)\left[a(k,\omega) + b(k,\omega)\sin 2\tau\right] = 0, \tag{14}$$

where

$$a(k,\omega) = \frac{2k^2}{\omega^2}\left(\frac{k^2}{2} + \sqrt{\frac{2}{\pi}}\frac{\rho g\Omega\left(q-3\right)^{3/2}\sqrt{(q-5)(1+q)}}{(q-5)\sqrt{(q-2)\left[g\rho(q-3)(1+q)+2\pi(q-5)\right]}}\right), \tag{15}$$

$$b(k,\omega) = \sqrt{\frac{2}{\pi}}\frac{2k^2\epsilon g\rho\Omega\left(q-3\right)^{3/2}\sqrt{(q-5)(1+q)}}{\omega^2(q-5)\sqrt{(q-2)\left[g\rho(q-3)(1+q)+2\pi(q-5)\right]}}, \tag{16}$$

and $\omega t = 2\tau$. The waves observed experimentally correspond to the most unstable solutions of equation (14) which, for small positive values of $b(k,\omega)$, are known from the stability analysis of Mathieu equations to be given by $a(k,\omega) = 1$ [41]. As for small values of $b(k,\omega)$ one can easily check that equation (14) has solutions of the form $\sin(\sqrt{a}\tau)$ and $\cos(\sqrt{a}\tau)$, the most unstable solutions have a frequency half that of the parametric drive and are usually referred to as Faraday waves. These waves have a long honored history which goes back to to Ernst Chladni's "beautiful series of forms assumed by sand, fillings, or other grains when lying upon vibrating plates" that "are so striking as to be recalled to the minds of those who have seen them by

the slightest reference", Hans Christian Ørsted's experiments with lycopodium light powders, and Michael Faraday's "crispations" seen in "fluids in contact with vibrating surfaces" [42]. The prototypical example of parametric wave amplification is that of a shallow contained filled with liquid that is oscillated in the vertical direction, a setting in which the acceleration periodically modulates the effective gravity and for drives of sufficiently large amplitudes a surface wave instability occurs with frequency one half that of the drive. The Faraday wave is the most unstable surface wave outside of the radial resonance, but in the vicinity of $\omega = \Omega$ the approximation for $w(t)$ breaks down, equation (14) includes the contribution of the higher harmonics (of very small amplitude) and a different surface wave emerges. This surface wave appears due to the resonant energy transfer [43] between the bulk of the condensate and the surface wave which sets $a(k,\omega) = 2^2$ such that the frequency with which the surface wave oscillates is equal with that of the radial breathing mode.

Solving analytically $a(k,\omega) = n^2$ one finds

$$\begin{aligned} k = & \Bigg\{ \sqrt{2} g (3-q)^{3/2} \Omega \rho \sqrt{-H(q)(1+q)(g\rho(3-q)(q-1)+2\pi(q-5))} \\ & - \Big[ H(q) \big( g\rho(q-3)(1+q)+2\pi(q-5) \big) \Big( 2g^2\Omega^2\rho^2(q-3)^3(1+q) \\ & + g n^2 \pi \rho \omega^2 H(q)(q-3)(1+q) + 2n^2\pi^2\omega^2(q-5)^2(q-2) \Big) \Big]^{1/2} \Bigg\}^{1/2} \\ & \times \Big( \pi^{1/4} H(q) \left[ g\rho(q-3)(1+q)+2\pi(q-5) \right] \Big)^{-1}, \end{aligned} \tag{17}$$

where $H(q) = (5-q)(2-q)$. Similar dispersion relations have been derived in Refs. [15, 16] for Faraday waves (that is, $n = 1$) by perturbing the ground state of a cigar-shaped BEC. These relations, however, rely on a wave function which is not normalized and does not minimize the Lagrangian, therefore the results are slightly fortuitous.

## 3. RESULTS

Solving numerically the equations (6)-(9) using a standard 4-5 embedded Runge-Kutta method we obtain the dynamics of the bulk of the condensate and that of the surface wave. Analyzing

$$A(t) = n(0,t) - n\left(\frac{\pi}{k}, t\right) \tag{18}$$

$$= \frac{4ku(t)}{\pi\left(2+u^2(t)+v^2(t)\right)}, \tag{19}$$

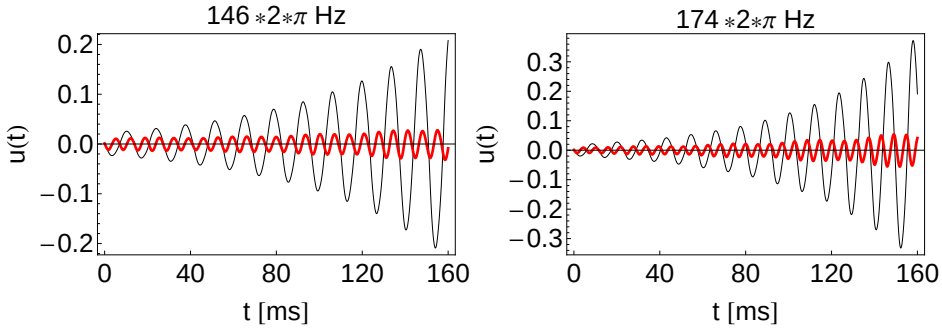


Fig. 1 – The dynamics of $u(t)$ for the Faraday and resonant wave in an experimental setup of $N = 5 \cdot 10^5$ atoms of $^{87}$Rb, $L = 180$ μm, $\Omega = 160.5(2\pi)$ Hz and $\epsilon = 0.1$ for $\omega = 146(2\pi)$ Hz and $\omega = 174(2\pi)$ Hz respectively. Notice in both figures that the Faraday wave emerges considerably faster than the resonant wave and exhibits an almost exponential blow-out.

where

$$n(z,t) = \int_0^{\frac{\sqrt{2}w(t)}{\sqrt{1-q}}} \mathrm{d}r 2\pi r \left|\psi\right|^2, \tag{20}$$

we see that $u(t)$ is a good indicator for the formation of the surface wave. Consequently, to analyze the emergence of the Faraday and the resonant wave we plot in Figs. 1–4 $u(t)$ for the two waves, straight on and in a vicinity of the radial resonance using a realistic experimental setup of $N = 5 \cdot 10^5$ atoms of $^{87}$Rb, $L = 180$ μm, $\Omega = 160.5(2\pi)$ Hz and $\epsilon = 0.1$. This setting corresponds to that used in Ref. [8], with the difference that we consider for simplicity a condensate with longitudinal homogeneity and compute the spatial extent of the condensate using a Thomas-Fermi approximation. The radial distribution was determined from the numerical solution of equation (5) which yields (to four digits) an equilibrium value $q = 0.0822$ that indicates that the condensate is well within the high-density regime [36].

The main message conveyed by Figs. 1-4 is that for modulation frequencies different from the radial trapping frequency the Faraday waves emerge faster than the resonant wave, while straight at resonance the resonant wave blows out exponentially and masks the Faraday wave. In a vicinity of the resonance the two waves have similar instability onset times.

Computing $s_F/s_R = k_R/k_F$ using equation (17), namely the ratio between the period of the Faraday wave and that of the resonant wave, one sees in Fig. 5 that for all frequencies of interest the period of the Faraday wave is roughly twice that of the resonant wave.

Let us emphasize that our model does not describe the real interplay between the two waves and only captures the formation of individual surface waves. In fact, the scattered experimental data reported in Ref. [8] for the observed period of the

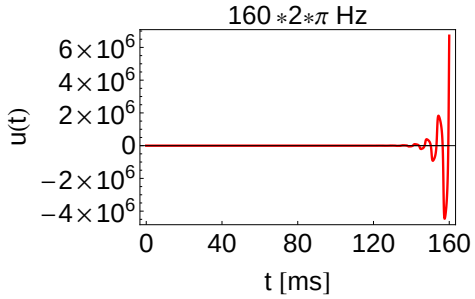


Fig. 2 – The dynamics of $u(t)$ for the Faraday and resonant wave for $\omega = 160(2\pi)$ Hz. Same experimental setup as in Fig. 1. Notice that the resonant wave emerges exponentially fast and it completely masks the Faraday wave. This behavior is typical for resonant forcing and is due to a resonant energy transfer between the collective mode of the bulk and the emergent surface wave.

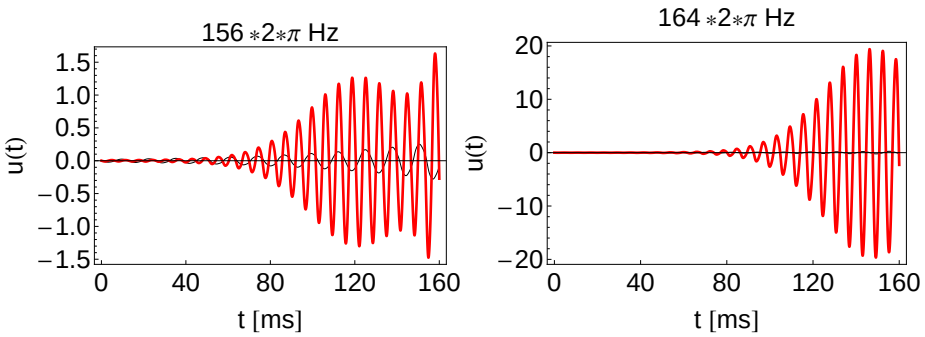


Fig. 3 – The dynamics of $u(t)$ for the Faraday and resonant wave for $\omega = 156(2\pi)$ Hz and $\omega = 164(2\pi)$ Hz respectively. Same experimental setup as in Fig. 1. Notice in both figures that the Faraday and the resonant wave have comparable instability onset-times, even though the resonant wave emerges somewhat faster. The two figures pertain to the scattered experimental data for the observed period of the surface wave before and after resonance that was reported in Ref. [8].

surface wave before and after resonance suggests the coexistence of the two waves, while our model only shows that the two waves have similar instability onset-times (see Fig. 4). A more realistic model should include two surface waves of arbitrary periods, but such a variational model yields a Whittaker-Hill-type equation for which the Floquet exponents (and therefore the unstable solutions) are not known analytically. The present variational model represents a trade off between the analytical tractability of the one-component surface wave and the accurate description of the dynamics of the bulk of the condensate.

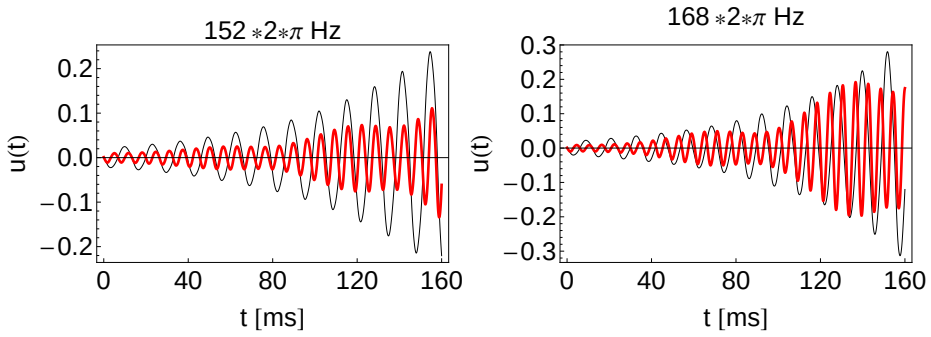


Fig. 4 – The dynamics of $u(t)$ for the Faraday and resonant wave for $\omega = 152(2\pi)$ Hz and $\omega = 168(2\pi)$ Hz respectively. Same experimental setup as in Fig. 1. Notice in both figures that the Faraday and resonant wave have similar instability onset-times and none of the waves has exponential blow-out.

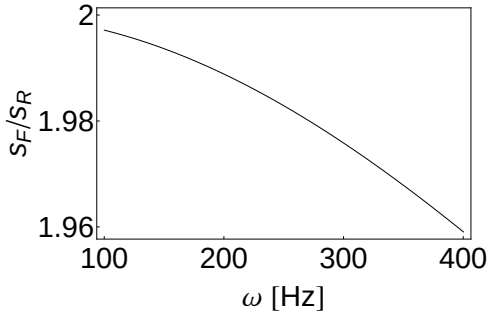


Fig. 5 – The ratio between the period of the Faraday wave and that of the resonant wave.

## 4. CONCLUSIONS

In conclusion we have shown by variational means that a cigar-shaped condensate subject to periodic modulation of the radial confinement will exhibit longitudinal Faraday waves for modulation frequencies different from the radial trapping frequency, while straight at resonance the resonant wave blows out exponentially and masks the Faraday wave. In a vicinity of the resonance the two wave have similar instability onset times and the existing experimental data suggests that the waves coexist. A more detailed experimental investigation of the resonant regime is needed and we suggest that the condensate is probed after 50 ms or so such that the surface wave is fully formed.

***Acknowledgements.*** The author thanks Virgil Băran, Mihnea Dulea, Antun Balaž, Dumitru Mihalache and Alex Nicolin for fruitful discussions over the past year. This work was supported in part by the European Commission under EU FP7 project HP-SEE (under contract number 261499) and ANCS project PN 09370104/2009.

REFERENCES


1. C.J. Pethick, H. Smith, *Bose-Einstein Condensation in Dilute Gases* (Cambridge University Press, Cambridge, 2008).
2. P.G. Kevrekidis, D.J. Frantzeskakis, R. Carretero-González (Eds.), *Emergent Nonlinear Phenomena in Bose-Einstein Condensates* (Springer-Verlag, Berlin, 2008); R. Carretero-González, D.J. Frantzeskakis, P.G. Kevrekidis, Nonlinearity **21**, R139 (2008).
3. D.J. Frantzeskakis, J. Phys. A: Math. Theor. **43**, 213001 (2010).
4. Y.V. Kartashov, B.A. Malomed, L. Torner, Rev. Mod. Phys. **83**, 247 (2011).
5. J.J. García-Ripoll, V.M. Pérez-García, P. Torres, Phys. Rev. Lett. **83**, 1715 (1999).
6. K. Staliunas, S. Longhi, G.J. de Valcárcel, Phys. Rev. Lett. **89**, 210406 (2002); K. Staliunas, S. Longhi, G.J. de Valcárcel, Phys. Rev. A **70**, 011601(R) (2004).
7. M. Kramer, C. Tozzo, F. Dalfovo, Phys. Rev. A **71**, 061602(R) (2005); C. Tozzo, M. Kramer, F. Dalfovo, Phys. Rev. A **72**, 023613 (2005); M. Modugno, C. Tozzo, F. Dalfovo, Phys. Rev. A **74**, 061601(R) (2006).
8. P. Engels, C. Atherton, M.A. Hoefer, Phys. Rev. Lett. **98**, 095301 (2007).
9. H. Abe, T. Ueda, M. Morikawa, Y. Saitoh, R. Nomura, and Y. Okuda, Phys. Rev. E **76**, 046305 (2007); T. Ueda, H. Abe, Y. Saitoh, R. Nomura and Y. Okuda, J. Low Temp. Phys. **148**, 553 (2007).
10. S.E. Pollack, D. Dries, R.G. Hulet, K.M.F. Magalhaes, E.A.L. Henn, E.R.F. Ramos, M.A. Caracanhas, V.S. Bagnato, Phys. Rev. A **81**, 053627 (2010).
11. I. Vidanović, A. Balaž, H. Al-Jibbouri, A. Pelster, Phys. Rev. A **84**, 013618 (2011).
12. A. Balaž, A. Bogojević, I. Vidanović, and A. Pelster, Phys. Rev. E **79**, 036701 (2009); I. Vidanović, A. Bogojević, A. Balaž, A. Belić, Phys. Rev. E **80**, 066706 (2009); A. Balaž, I. Vidanović, A. Bogojević, and A. Pelster, Phys. Lett. A **374**, 1539 (2010); A. Balaž, I. Vidanović, A. Bogojević, A. Belić, and A. Pelster, J. Stat. Mech., P03004 (2011); A. Balaž, I. Vidanović, A. Bogojević, A. Belić, and A. Pelster, J. Stat. Mech., P03005 (2011).
13. N. Katz and O. Agam, New J. Phys. **12**, 073020 (2010).
14. K. Staliunas, Phys. Rev. A **84**, 013626 (2011).
15. A.I. Nicolin, R. Carretero-González, and P.G. Kevrekidis, Phys. Rev. A **76**, 063609 (2007).
16. A.I. Nicolin, M.C. Raportaru, Physica A **389**, 4663 (2010).
17. R. Nath, L. Santos, Phys. Rev. A **81**, 033626 (2010).
18. O. Morsch, M. Oberthaler, Rev. Mod. Phys. **78**, 179 (2006).
19. B. Wu and Q. Niu, Phys. Rev. A **61**, 023402 (2000); B. Wu, R.B. Diener, and Q. Niu, Phys. Rev. A **65**, 025601 (2002).
20. D. Diakonov, L.M. Jensen, C.J. Pethick, H. Smith, Phys. Rev. A **66**, 013604 (2002); M. Machholm, C.J. Pethick, H. Smith, Phys. Rev. A **67**, 053613 (2003); M. Machholm, A. Nicolin, C.J. Pethick, H. Smith, Phys. Rev. A **69**, 043604 (2004).
21. P. Capuzzi, M. Gattobigio, P. Vignolo, Phys. Rev. A **83**, 013603 (2011).
22. P. Capuzzi, P. Vignolo, Phys. Rev. A **78**, 043613 (2008).
23. R.A. Tang, H.C. Li, J.K. Xue, J. Phys. B: At. Mol. Opt. Phys. **44**, 115303 (2011).
24. C.D. Graf, G. Weick, E. Mariani, EPL **89**, 40005 (2010).
25. D. Mihalache, D. Mazilu, L. Torner, Phys. Rev. Lett. **81**, 4353 (1998); D. Mihalache, D. Mazilu, L.-C. Crasovan, L. Torner, B.A. Malomed, F. Lederer, Phys. Rev. E **62**, 7340 (2000); I.V. Mel'nikov, D. Mihalache, N.-C. Panoiu, Opt. Commun. **181**, 345 (2000); D. Mihalache, D. Mazilu, L.-C. Crasovan, B.A. Malomed, F. Lederer, L. Torner, Phys. Rev. E **68**, 046612 (2003); D. Mihalache, D. Mazilu, F. Lederer, Y.S. Kivshar, Opt. Express **15**, 589 (2007); H. Leblond, B.A. Malomed,

D. Mihalache, Phys. Rev. A **83**, 063825 (2011).

26. L.-C. Crasovan, B.A. Malomed, D. Mihalache, Phys. Lett. A **289**, 59 (2001); L.-C. Crasovan, B.A. Malomed, D. Mihalache, Phys. Rev. E **63**, 016605 (2001); V. Skarka, N.B. Aleksic, H. Leblond, B.A. Malomed, D. Mihalache, Phys. Rev. Lett. **105**, 213901 (2010); D. Mihalache, Proc. Romanian Acad. A **11**, 142 (2010); D. Mihalache, Rom. Rep. Phys. **63**, 9 (2011); D. Mihalache, Rom. Rep. Phys. **63**, 325 (2011).
27. B.A. Malomed, D. Mihalache, F. Wise, L. Torner, J. Opt. B: Quantum Semiclass. Opt. **7**, R53 (2005).
28. S.K. Adhikari, Phys. Rev. E **62**, 2937 (2000); S.K. Adhikari, Phys. Lett. A **265**, 91 (2000); S.K. Adhikari, P. Muruganandam, J. Phys. B: At. Mol. Opt. **35**, 2831 (2002); S.K. Adhikari, P. Muruganandam, J. Phys. B: At. Mol. Opt. **36**, 2501 (2003); P. Muruganandam, S.K. Adhikari, Comp. Phys. Comm. **180**, 1888 (2009).
29. L. Salasnich, A. Parola, L. Reatto, Phys. Rev. A **65**, 043614 (2002); L. Salasnich, Laser Phys. **12**, 198 (2002); L. Salasnich, J. Phys. A: Math. Theor. **42**, 335205 (2009); A.I. Nicolin, Rom. Rep. Phys. **61**, 641 (2009).
30. A. Muñoz Mateo and V. Delgado, Phys. Rev. A **75**, 063610 (2007); A. Muñoz Mateo, V. Delgado, Phys. Rev. A **77**, 013607 (2008); A. Muñoz Mateo, V. Delgado, Ann. Phys. **324**, 709 (2009).
31. A. Smerzi, A. Trombettoni, Chaos **13**, 766 (2003); A. Smerzi, A. Trombettoni, Phys. Rev. A **68**, 023613 (2003).
32. V.M. Pérez-García, H. Michinel, J.I. Cirac, M. Lewenstein, P. Zoller, Phys. Rev. Lett. **77**, 5320 (1996); V.M. Pérez-García, H. Michinel, J.I. Cirac, M. Lewenstein, P. Zoller, Phys. Rev. A **56**, 1424 (1997); A.I. Nicolin, Rom. Rep. Phys. **63**, 187 (2011).
33. A.L. Fetter, J. Low. Temp. Phys. **106**, 643 (1997).
34. K.S. Fa, R.S. Mendes, P.R.B. Pedreira, E.K. Lenzi, Physica A **295**, 242 (2001).
35. E. Erdemir, B. Tanatar, Physica A **322**, 449 (2003).
36. A.I. Nicolin, R. Carretero-González, Physica A **387**, 6032 (2008).
37. A.I. Nicolin, M.C. Raportaru, Proc. Romanian Acad. A **12**, 209 (2011).
38. A.I. Nicolin, Phys. Rev. E **84**, 056202 (2011).
39. A.I. Nicolin, Rom. Rep. Phys. **63**, 1329 (2011); A.I. Nicolin, Physica A **391**, 1062 (2012); A. Balaž, A.I. Nicolin, Phys. Rev. A **85**, 023613 (2012).
40. A. Gubeskys, B.A. Malomed, I.M. Merhasin, Stud. Appl. Math. **115**, 255 (2005).
41. N.W. McLachlan, *Theory and Application of Mathieu Functions* (Oxford Univ. Press, New York, 1951).
42. M. Faraday, Philos. Trans. R. Soc. London **121**, 299 (1831).
43. A.I. Nicolin, M.H. Jensen, R. Carretero-González, Phys. Rev. E **75**, 036208 (2007); A.I. Nicolin, M.H. Jensen, J.W. Thomsen, R. Carretero-González, Physica D **237**, 2476 (2008).